

# Determination of concerted or stepwise mechanism of hydrogen tunneling from isotope effects: Departure between experiment and theory

Cite as: J. Chem. Phys. **156**, 124304 (2022); <https://doi.org/10.1063/5.0085010>

Submitted: 11 January 2022 • Accepted: 04 March 2022 • Accepted Manuscript Online: 04 March 2022  
• Published Online: 23 March 2022

 Yi-Han Cheng,  Yu-Cheng Zhu,  Wei Kang, et al.



View Online



Export Citation



CrossMark

## ARTICLES YOU MAY BE INTERESTED IN

[Chlorine dioxide: An exception that proves the rules of localized chemical bonding](#)

The Journal of Chemical Physics **156**, 124303 (2022); <https://doi.org/10.1063/5.0084739>

[Photodissociation dynamics of  \$N\_3^+\$](#)

The Journal of Chemical Physics **156**, 124307 (2022); <https://doi.org/10.1063/5.0085081>

[Kinetic Monte Carlo simulations for heterogeneous catalysis: Fundamentals, current status, and challenges](#)

The Journal of Chemical Physics **156**, 120902 (2022); <https://doi.org/10.1063/5.0083251>

Lock-in Amplifiers  
up to 600 MHz



Zurich  
Instruments



# Determination of concerted or stepwise mechanism of hydrogen tunneling from isotope effects: Departure between experiment and theory

Cite as: J. Chem. Phys. 156, 124304 (2022); doi: 10.1063/5.0085010

Submitted: 11 January 2022 • Accepted: 4 March 2022 •

Published Online: 23 March 2022



View Online



Export Citation



CrossMark

Yi-Han Cheng,<sup>1</sup> Yu-Cheng Zhu,<sup>1,a)</sup> Wei Kang,<sup>2</sup> Xin-Zheng Li,<sup>1,3,4,5</sup> and Wei Fang<sup>6,7,b)</sup>

## AFFILIATIONS

<sup>1</sup> State Key Laboratory for Artificial Microstructure and Mesoscopic Physics, Frontier Science Center for Nano-optoelectronics and School of Physics, Peking University, Beijing 100871, China

<sup>2</sup> College of Engineering, Peking University, Beijing 100871, People's Republic of China

<sup>3</sup> Interdisciplinary Institute of Light-Element Quantum Materials and Research Center for Light-Element Advanced Materials, Peking University, Beijing 100871, China

<sup>4</sup> Peking University Yangtze Delta Institute of Optoelectronics, Nantong, Jiangsu 226010, China

<sup>5</sup> Collaborative Innovation Center of Quantum Matter, Peking University, Beijing 100871, People's Republic of China

<sup>6</sup> State Key Laboratory of Molecular Reaction Dynamics and Center for Theoretical Computational Chemistry, Dalian Institute of Chemical Physics, Chinese Academy of Sciences, Dalian 116023, People's Republic of China

<sup>7</sup> Department of Chemistry, Fudan University, Shanghai 200438, People's Republic of China

<sup>a)</sup> Electronic mail: zhuyucheng@pku.edu.cn

<sup>b)</sup> Author to whom correspondence should be addressed: wei.fang.13@alumni.ucl.ac.uk

## ABSTRACT

Isotope substitution is an important experimental technique that offers deep insight into reaction mechanisms, as the measured kinetic isotope effects (KIEs) can be directly compared with theory. For multiple proton transfer processes, there are two types of mechanisms: stepwise transfer and concerted transfer. The Bell–Limbach model provides a simple theory to determine whether the proton transfer mechanism is stepwise or concerted from KIEs. Recent scanning tunneling microscopy (STM) experiments have studied the proton switching process in water tetramers on NaCl(001). Theoretical studies predict that this process occurs via a concerted mechanism; however, the experimental KIEs resemble the Bell–Limbach model for stepwise tunneling, raising questions on the underlying mechanism or the validity of the model. We study this system using *ab initio* instanton theory, and in addition to thermal rates, we also considered microcanonical rates, as well as tunneling splittings. The instanton theory predicts a concerted mechanism, and the KIEs for tunneling rates (both thermal and microcanonical) upon deuteration are consistent with the Bell–Limbach model for concerted tunneling but could not explain the experiments. For tunneling splittings, partial and full deuteration change the size of it in a similar fashion to how they change the rates. We further examined the Bell–Limbach model in another system, porphycene, which has both stepwise and concerted tunneling pathways. The KIEs predicted by instanton theory are again consistent with the Bell–Limbach model. This study highlights differences between KIEs in stepwise and concerted tunneling and the discrepancy between theory and recent STM experiments. New theory/experiments are desired to settle this problem.

Published under an exclusive license by AIP Publishing. <https://doi.org/10.1063/5.0085010>

## I. INTRODUCTION

Hydrogen bonding is ubiquitous in the gas phase clusters, on surfaces, and in condensed matter.<sup>1–4</sup> The small mass of

hydrogen (H) means that many properties of the H-bonded systems are quantum mechanical in nature.<sup>5–7</sup> The associated nuclear quantum effects (NQE), which refer to the differences between properties of a realistic system when the nuclei are

described as quantum or classical particles, can be reflected by many phenomena, e.g., quantum delocalization of H, quantum tunneling, and zero-point energies effects.<sup>8</sup> Theoretically, developments of *ab initio* computer simulation methods in recent years have demonstrated the importance of NQEs in many systems, e.g., water nanostructures on metal surfaces,<sup>9</sup> ice,<sup>3,4,8,10–12</sup> and organic molecules.<sup>13–17</sup> From the experimental perspective, techniques such as nuclear magnetic resonance (NMR) measurements in gas phase systems,<sup>18,19</sup> high-resolution scanning tunneling microscopy (STM) on surfaces,<sup>20–22</sup> helium scattering on surfaces,<sup>23</sup> sum-frequency generation (SFG) spectroscopy for interfaces,<sup>24–26</sup> and x-ray diffraction in solids<sup>27</sup> have provided valuable experimental data for the calibration of the theoretical methods and models. Due to progress from these two aspects, our understandings of NQEs in H-bonded systems have improved tremendously in recent years.

Isotope substitution, e.g., replacing H by deuterium (D), has played a crucial role in making theoretical simulations and experimental observations comparable. In chemical reactions, a key quantity related to this is the kinetic isotope effect (KIE), which refers to the changes in the chemical reaction rates when one of the elements in the reactants is substituted by one of its isotopes. KIEs can be directly measured in experiments. Theoretically, it is primarily a quantum mechanical property since (i) heavier isotopologue has smaller vibrational frequencies compared to its lighter counterpart, resulting in different zero-point energies, and (ii) if quantum tunneling occurs, the probability of the system passing through a potential energy barrier decreases with the square root of the effective mass. Therefore, KIEs normally increase with decreasing temperature ( $T$ ).<sup>28</sup> This is especially true in the deep tunneling regime, and a prominent example of this resides on H/D diffusion on metal surfaces, where quantum tunneling of H/D plays a central role.<sup>23,29,30</sup> The microscopic details of these processes have been relatively well-understood.<sup>31</sup> In H-bonded systems, proton transfer (PT) processes can be more complicated because multiple protons can be involved. It can happen that each proton moves separately, which means that the process occurs in a “stepwise” manner. Meta-stable intermediate states (ISs) may also exist in stepwise PT, resulting in the existence of multiple transition states (TSs). It can also happen that the protons transfer collectively, commonly referred to as the “concerted” mechanism, and the process has only a single TS. Therefore, compared with single proton tunneling,<sup>29,31,32</sup> despite the numerous theoretical and experimental efforts exerted on multiple proton tunneling, our understanding of these processes is still lacking.

In this study, we investigate tunneling in processes involving multiple PTs, using the ring-polymer instanton theory<sup>33–37</sup> with on-the-fly *ab initio* calculations. We choose the KIEs and the tunneling splitting factors as the key quantities to analyze. Two systems are studied in this work: (i) water tetramer on NaCl(001), featuring a concerted tunneling mechanism,<sup>38</sup> and (ii) gas phase porphycene, featuring both concerted and stepwise (with meta-stable ISs) mechanisms. A simple theory exists for predicting KIEs in stepwise and concerted PT processes, known as the Bell–Limbach model,<sup>39,40</sup> which was established based on early NMR measurements. It states that the tunneling rate drops to similar values upon partial and full deuteration in stepwise tunneling scenario, while in the concerted scenario, the tunneling rate continues to drop significantly as the

system goes from partial to full deuteration. Our simulations for both systems agree qualitatively with this model. These consistent results, however, are inconsistent with recent high resolution cryogenic STM measurements for water tetramer on Au supported NaCl(001)<sup>21</sup> and for porphycene on Ag(110).<sup>20</sup> We also considered the possibility that a microcanonical rate, rather than a thermal rate, was measured in the experiments due to the low temperature and possible energy excitation caused by the electric current. The results show that the conflict between theory and experiments is not due to energy excitation. Besides KIEs, tunneling splitting may serve as an alternative experimental observable. Partial and full deuteration change the sizes of the splitting associated with the concerted tunneling channel in a way similar to that of the rates in the Bell–Limbach model. Overall, this study emphasizes some fundamental differences between the atomic level details of the stepwise and concerted tunneling mechanisms and their consequences. To achieve consensus on multiple proton tunneling, new experiments and theoretical simulations are still highly desired in future studies.

## II. METHODS

Transition-state theory (TST)<sup>41</sup> has been greatly successful in estimating the rate of chemical reactions. The classical TST rate is given by

$$k_{\text{TST}} = A_{\text{TST}} e^{-\beta V_{\text{TS}}}, \quad (1)$$

where  $V_{\text{TS}}$  is the energy of the TS with respect to the reactant,  $\beta = \frac{1}{k_{\text{B}}T}$ , and  $A_{\text{TST}}$  is a prefactor, which contains contributions from the partition functions. This TST rate is purely based on classical mechanics, and the Eyring TST rate adds partial quantum corrections [namely, zero-point energy (ZPE) corrections] heuristically by swapping out classical vibrational partition functions for quantum mechanical ones.

### A. Thermal ring-polymer instanton rate theory

Instanton theory<sup>35–37,42,43</sup> provides a computationally efficient method for computing tunneling rates via locating optimal tunneling pathways (called instantons). There are several different approaches to instanton theory as well as different implementations of it.<sup>33,37,44–49</sup> Instantons (under the ring-polymer representation) can be viewed as a quantum analog to the classical TST, and the instanton rate can be formally expressed in a form similar to Eq. (1),

$$k_{\text{inst}}(\beta) = A_{\text{inst}} e^{-S_{\text{inst}}[x(\tau)]/\hbar}. \quad (2)$$

The Euclidean action of an instanton is defined as

$$S_{\text{inst}}[x(\tau)] = \int_0^{\beta\hbar} \left[ \frac{1}{2} m |\dot{x}(\tau)|^2 + V(x(\tau)) \right] d\tau, \quad (3)$$

where the “instanton,”  $x(\tau)$ , is a cyclic path in imaginary time of length  $\beta\hbar$  traversing the barrier region. The prefactor  $A_{\text{inst}}$  contains

fluctuations around the instanton path described by its partition function. Making use of the discrete path-integral, instanton can be described in a ring-polymer form.<sup>33</sup> Being an optimal tunneling pathway that minimizes the Euclidean action, instantons can be located via 1st order saddle point optimization in an extended ring-polymer space. It can be obtained using methods similar to locating the transition state in a classical TST rate calculation. When  $T$  is lower than the crossover temperature<sup>50,51</sup>  $T_c \sim \frac{\hbar\omega_{TS,0}}{2\pi k_B}$ ,  $\omega_{TS,0}$  is the imaginary frequency of the TS, the ring-polymer instanton spreads out along the reaction coordinate. Its action  $S_{\text{inst}}/\beta < \hbar V_{\text{TS}}$ , meaning that the exponential part of the instanton rate becomes larger than that of the classical TST rate.

## B. Microcanonical instanton theory

Instanton theory can also be used to compute rates in the microcanonical ensemble, which is the reaction rate at a given reactant energy. The microcanonical rate constant is defined by<sup>52,53</sup>

$$k(E) = \frac{1}{2\pi\hbar} \frac{N(E)}{\rho_r(E)}, \quad (4)$$

where  $N(E)$  is the cumulative reaction probability for a system with total energy  $E$  (e.g., for the water tetramer on the NaCl system,  $E$  is the vibrational energy since the system does not translate nor rotate) and  $\rho_r(E)$  is the reactant density of states.

The key quantity in Eq. (4),  $N(E)$ , can be computed from instanton trajectories, and there are more than one formulation.<sup>42,46,54,55</sup> In this work, we use the density-of-states (DoS) instanton theory,<sup>56</sup> which is based on the summation formulation of Miller,<sup>54</sup> while made practical for large systems. Since we are computing microcanonical properties, it would be helpful to label each instanton using its energy instead of its imaginary time  $\tau$ . The instanton energy is defined as

$$E_I = \frac{\partial S}{\partial \tau}. \quad (5)$$

One first optimizes a series of instanton with different  $\tau$  values, corresponding to different values of  $E_I$ . We can define the DoS of each instanton, namely,  $\rho_I(E; E_I)$ , using Laplace transform,

$$\int_{E_I}^{\infty} dE \rho_I(E; E_I) e^{-\beta E} = Z_I(\tilde{\beta}; E_I) e^{-\tilde{\beta} E_I}, \quad (6)$$

where  $\tilde{\beta}$  is the Laplace transformation variable,  $Z_I$  is the partition function of the instanton (note that this is not the same as the ring-polymer partition function; for details, please see Ref. 56). By making the steepest-descent approximation to the inverse Laplace transform, one can practically compute  $\rho_I(E; E_I)$  for each instanton,

$$\rho_I(E; E_I) = \left( 2\pi \frac{\partial^2 \ln[Z_I(\tilde{\beta}; E_I) e^{-\tilde{\beta} E_I}]}{\partial \tilde{\beta}^2} \right)^{-\frac{1}{2}} e^{\tilde{\beta} E} Z_I(\tilde{\beta}; E_I) e^{-\tilde{\beta} E_I}, \quad (7)$$

$$E(\tilde{\beta}) = -\frac{\partial \ln[Z_I(\tilde{\beta}; E_I) e^{-\tilde{\beta} E_I}]}{\partial \tilde{\beta}}.$$

Then,  $N(E)$  in the DoS formulation is given by

$$N_{\text{DoS}}(E) = \int_{E_{\text{min}}}^{\infty} dE_I P_{\text{SC}}(E_I) \rho_I(E; E_I), \quad (8)$$

where  $P_{\text{SC}}$  is the semiclassical transmission probability, and in this work, we use the expression with the parabolic top correction,<sup>46,57</sup>

$$P_{\text{SC}}(E) = \begin{cases} [1 + e^{W(E)/\hbar}]^{-1}, & E < V_{\text{TS}}, \\ [1 + e^{W_{\text{pb}}(E)/\hbar}]^{-1}, & E \geq V_{\text{TS}}, \end{cases} \quad (9)$$

where  $W$  is the abbreviated action  $W(E) = 2 \int \sqrt{2[V(g) - E]} dg$ ,  $g$  is the mass-weighted coordinate, and  $W_{\text{pb}}(E) = 2\pi(V_{\text{TS}} - E)/\omega_{\text{TS},0}$ . For more details of microcanonical instanton theory and the DoS instanton method, please refer to Ref. 56.

## C. Instanton theory for tunneling splittings

In a symmetric double-well system, overlap of the wavefunction of the two wells by tunneling will result in splitting of energy levels. The splitting size of the ground-state determined by the coupling strength, i.e., tunneling probability, is a  $T$ -independent quantity as it does not involve any thermal population of excited vibrational states. In the  $T \rightarrow 0$  limit, with the contribution of excited levels neglected,<sup>58</sup> one has

$$\begin{aligned} \lim_{\beta \rightarrow \infty} \frac{Q(\beta)}{2Q_0(\beta)} &= \lim_{\beta \rightarrow \infty} \frac{e^{-\beta(E_0 - \Delta/2)} + e^{-\beta(E_0 + \Delta/2)}}{2e^{-\beta E_0}} \\ &= \lim_{\beta \rightarrow \infty} \cosh\left(\frac{\beta \Delta}{2}\right), \end{aligned} \quad (10)$$

where  $Q(\beta)$  ( $2Q_0(\beta)$ ) is the partition function of the double-well system (two unconnected single wells).  $E_0 \pm \Delta/2$  are the energy levels split by tunneling.  $Q_0(\beta)$  can be evaluated simply by the vibrational frequencies of a well.

Applying the method of steepest-descent,  $Q(\beta)$  can be approximated by instantons. Specially, in the  $T \rightarrow 0$  limit, the instanton trajectory is quite different from that at finite  $T$ . It spends most time staying in the wells and pass the barrier occasionally. A pass process is quick, called a ‘‘kink,’’<sup>51</sup> and it can happen arbitrary (even) times because the imaginary time of the path ( $\beta\hbar$ ) is infinite. If the number of kinks is zero, the instanton is collapsed in the reactant well and its partition function reduces to  $Q_0$ .

Enumerating all possible instanton trajectories, one arrives at

$$Q(\beta) = \sum_{n=0, \text{even}}^{\infty} \frac{2N^n}{n!} Q_n(\beta), \quad (11)$$

where  $Q_n(\beta)$  represents the contribution from a trajectory containing  $n$  kinks. The prefactor is the number of ways of arranging  $n$  kinks in a ring-polymer of  $N$  beads. In the  $N \rightarrow \infty$  limit, all the kinks can be viewed as isolated and identical kinks. With the contribution from the trivial beads (i.e., beads that are collapsed in a well),  $Q_0$ , excluded,  $Q_n(\beta)$  is only related to  $n$  and the contribution of one kink (donated as  $\theta$ ) through

$$\frac{Q_n}{Q_0} = \theta^n. \quad (12)$$

$\theta$  can be calculated from a *linear* polymer composed of finite beads connecting the two wells.

Combining the above equations, one can get the final expression for the ground-state tunneling splitting of a double-well system,

$$\Delta = \frac{2}{\beta_N} \theta = \frac{2\hbar}{\Phi} \sqrt{\frac{S_{\text{kink}}}{2\pi\hbar}} e^{-S_{\text{kink}}/\hbar}. \quad (13)$$

$S_{\text{kink}}$  is the Euclidean action of the kink described by a linear polymer and  $\Phi$  is the fluctuation term. Both quantities are  $T$ -independent. For more details of the linear polymer, please refer to Ref. 58.

#### D. Reducing the computational cost of instanton optimization with machine learning

In our simulations, we combine first-principles and machine learning (ML) methods to optimize instantons with a large number of beads at an affordable computational cost. The Gaussian process regression (GPR) method is employed to fit the potential-energy surface locally around the dominant tunneling pathway. This method can accelerate the convergence of instanton optimizations, significantly reducing the number of on-the-fly *ab initio* calculations required.<sup>59,60</sup> GPR models are trained using potential energies, gradients, and hessian data from density functional theory (DFT) calculations. We adapted the procedure described in Ref. 59, with some changes, mainly in that we first perform on-the-fly instanton optimizations with a small number of beads, and build our initial dataset from that. In specific, the initial GPR model is trained using potential energy, gradients from the optimized instanton, and five Hessians picked from the instanton trajectory. Then, the instanton is optimized with a large number of beads on the GPR potential energy surface. Then, we perform *ab initio* calculations on the GPR optimized instanton to obtain new gradients and potential energy data. If the gradients are not converged, we use the new DFT data as the training set (with the addition of a few hessian data computed on selected points on the GPR optimized instanton). We iterate this process until the instanton is converged. The Cartesian coordinates are used as the descriptor for this system because the system is not in the gas-phase, so internal coordinate descriptors cannot be directly applied.

### III. RESULTS

#### A. Water tetramer on Au supported NaCl(001)

We start discussions with water tetramer on Au supported NaCl(001), a system with one single TS for concerted tunneling. Two chirality states of the water tetramer exist, i.e., the clockwise state (CS) and the anti-clockwise state (AS) (see insets in Fig. 1). According to previous STM experiments, the Cl-terminated tip is positioned slightly off the center of the water tetramer. The switching dynamics of water tetramer chirality was monitored by recording the tunneling current as a function of time. When the tip is far above the water tetramer, the current remains constant, indicating no switching between the two chiral states. Once the tip height is reduced, two current levels appear, in addition to a sudden increase in the tunneling current. The low and high current levels can be assigned to the CS and the AS, respectively. The switching rate between them can be measured, which appears to be  $T$ -independent

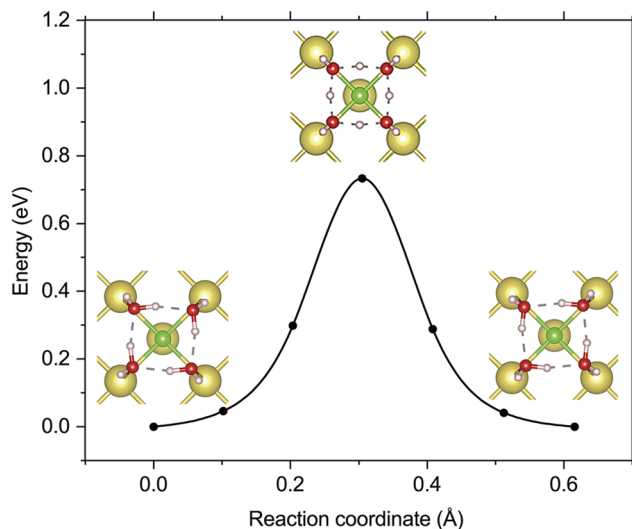


**FIG. 1.** MEP for chirality switching in the water tetramer on NaCl. The reaction coordinate is defined as the average distance the four hydrogens traveled from the CS minimum. The insets show structures of CS, AS, and TS.

at low  $T$ s, indicating that deep tunneling occurs.<sup>21</sup> To investigate how KIEs affect tunneling rates, full and partial isotopic substitutions on the chirality switching of a water tetramer have been performed.<sup>61</sup> The chirality switching rate of the  $4\text{H}_2\text{O}$  tetramer is substantially reduced by replacing only one  $\text{H}_2\text{O}$  with  $\text{D}_2\text{O}$ , to almost the same level as the  $4\text{D}_2\text{O}$  tetramer.<sup>61</sup>

To understand this, atomistic details of the chirality switching between CS and AS have been studied using classical and quantum theories. The transfer of a single proton from its donor to its acceptor necessarily creates defects and charge separations, and the large energy penalty associated with the transfer eliminates the possibility of sequential PT in chiral cyclic water tetramers at low  $T$ s. Concerted transfer of all four protons along their respective hydrogen bonds prevents the creation of charge defects,<sup>62</sup> therefore, becomes the only possible mechanism. So far, theoretical studies based on the analysis of NMR experiments have established a simple picture of the KIEs for stepwise and concerted tunneling, known as the Bell–Limbach tunneling model.<sup>40</sup> The KIE of the rate constant,  $k_{\text{LL}}$  ( $L = \text{H}$  or  $\text{D}$ ), in the tunneling regime, follows,

$$k_{\text{HH}} \gg k_{\text{HD}} \approx 2k_{\text{DD}} \quad (14)$$

for the stepwise mechanism and

$$k_{\text{HH}}/k_{\text{HD}} \approx k_{\text{HD}}/k_{\text{DD}} \quad (15)$$

for the concerted one.<sup>39,40</sup> The Bell–Limbach tunneling model have also been extended to describe the multiple PT process with more than two protons.<sup>63</sup> For example, for the water tetramer system, the relation between transfer rates with four transferring H atoms ( $k_{4\text{H}}$ ), three H and one D ( $k_{3\text{H}1\text{D}}$ ), and four D atoms ( $k_{4\text{D}}$ ) satisfies

$$(k_{4\text{H}}/k_{3\text{H}1\text{D}})^3 \approx k_{3\text{H}1\text{D}}/k_{4\text{D}}, \quad (16)$$

if the underlying mechanism is concerted. A previous simulation study<sup>61</sup> using rate theory based on *ab initio* ring-polymer

molecular dynamics<sup>64,65</sup> has computed the KIEs at low temperatures. We find that the previous results show behavior in qualitative agreement with Eq. (16), consistent with the fact that only the concerted tunneling channel is available.<sup>61</sup> The experimental KIE results<sup>61</sup> show that  $k_{4H}$  is 1–2 orders of magnitude higher than  $k_{3H1D}$ , and that  $k_{3H1D} \approx k_{4D}$ , which obviously do not satisfy Eq. (16).

To investigate the KIEs on the tunneling rates efficiently, we use *ab initio* instanton theory, with the electronic structure computed on-the-fly with DFT. Tunneling splitting, a quantity neglected in previous studies, is also analyzed. The DFT calculations are performed using the Vienna *Ab initio* Simulation Package (VASP),<sup>66,67</sup> together with projector augmented wave (PAW) pseudopotentials and a cutoff energy of 800 eV for the expansion of the electronic wave functions. The exchange–correlation interactions are described within the generalized gradient approximation (GGA), using the Perdew–Burke–Ernzerhof (PBE) functional.<sup>68</sup> Dispersion interactions are accounted for using the DFT-D2 method.<sup>69</sup> We use a bilayer NaCl substrate in a  $2 \times 2$  unit cell (with 18 atoms per layer). The thickness of the vacuum above the slab is 10 Å. The Brillouin zone is sampled using a  $(2 \times 2 \times 1)$  Gamma centered Monkhorst–Pack k-point mesh. The substrate is kept fixed during the instanton optimizations. We have checked that substrate relaxation only has a small impact on the reaction barrier. We use the climbing image nudged elastic band (cNEB) method<sup>70</sup> to obtain the potential energy profiles of concerted proton transfer, with the maximum force converged to below 0.01 eV/Å. The potential energy profile (Fig. 1) shows the minimum energy pathway (MEP) for the chirality switching of the collective proton transfer, with a barrier of  $\sim 0.73$  eV.

The crossover temperatures ( $T_c$ ) of the  $4H_2O$ ,  $3H_2O + D_2O$ , and  $4D_2O$  systems are 327, 303, and 234 K, respectively, indicating that tunneling can occur even at moderately high  $T$ s. To explore the  $T$ -dependence of the switching rates, we study the tunneling rates of the water tetramer at a wide range of  $T$ s (from 200 down to 50 K). Our instanton calculations use 50 beads at 250 K and an increasing number of beads at lower temperatures (up to 170 beads for 100 K and below), with the *total force* on the instanton converged to below 0.06 eV/Å. The geometries of the optimized instanton paths at a moderate  $T$  (200 K) and a low  $T$  (80 K) are shown in Fig. 2. At 200 K [Figs. 2(a)–2(c)], the tunneling distance (indicated by the instanton path length of the transferring hydrogen atoms) is very short for  $4D_2O$ . The instanton for the  $3H_2O + D_2O$  system resembles that of the  $4H_2O$  system, and the tunneling distance is obviously longer than in the  $4D_2O$  system. All the instantons become more delocalized (i.e., the length of the instanton path increases) as  $T$  decreases, indicating a gradual transition to deep tunneling. The long instanton path at 80 K suggests that concerted proton transfers happen through deep tunneling at this  $T$ . The instanton pathway deviates from the classical pathway (i.e., MEP), which is an effect known as “corner-cutting.”<sup>75,74</sup> As  $T$  decreases, corner-cutting effects become more apparent (Fig. 2), which is an interesting feature of this system as tunneling (even deep tunneling) is not necessarily accompanied by corner-cutting.<sup>49</sup> The hydrogen atoms in the instanton tunnel via a more straight path, rather than traveling a longer curved path as in the MEP, in order to reduce tunneling distance. In addition, the heavier O atoms barely tunnel in the instanton, whereas they move significantly in the MEP. This indicates that the chirality switching

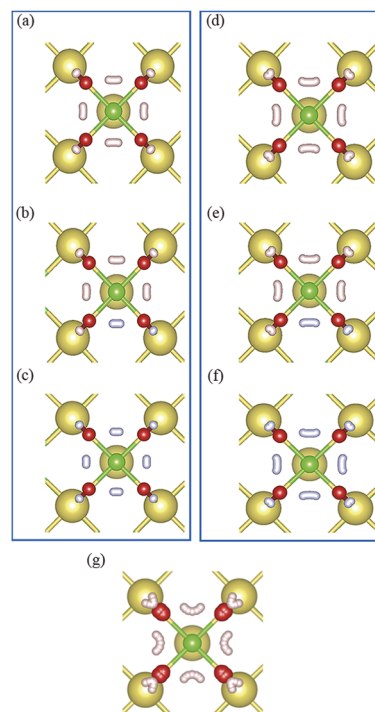


**FIG. 2.** Comparison of instanton paths and the MEP. [(a)–(c)] Geometry of the instanton paths for  $4H_2O$ ,  $3H_2O + D_2O$ , and  $4D_2O$  at 200 K. [(d)–(f)] Geometry of the instanton paths at 80 K. (g) Geometry of the MEP. O, H, D, Na, and Cl atoms are colored red, light pink, light blue, yellow, and green, respectively.

via deep tunneling does not require the contraction of the O atoms in the water tetramer. The “on-the-fly” instanton method used in this work provides a practical way to study multi-dimensional tunneling effects such as the “corner-cutting” effects observed here.

The instanton rates at different temperatures are shown in Fig. 3(a). At high  $T$ s, the instanton rates are close to the Eyring TST rates. As  $T$  decreases, contributions from quantum tunneling to the rates increase, showing a strong non-Arrhenius behavior. The KIEs also increase with decreasing temperature and become weakly temperature dependent at low  $T$ s. This trend agrees qualitatively with previous PIMD calculations.<sup>61</sup> The thermal instanton rates show that partial deuteration leads to two orders of magnitude decrease in the switching rates, which is consistent with previous STM experiments and PIMD simulations. For full deuteration, however, our simulations show that the rate decreases much more than partial deuteration, consistent with previous theoretical predictions but inconsistent with previous experimental results. In fact, the relation between the instanton rates is consistent with the Bell–Limbach model [Eq. (16)]. We note that the PBE functional may underestimate the potential energy barrier for this system due to self-interaction errors. Our tests using a hybrid functional (HSE06) show that self-interaction errors do not have any qualitative impact on our findings here.

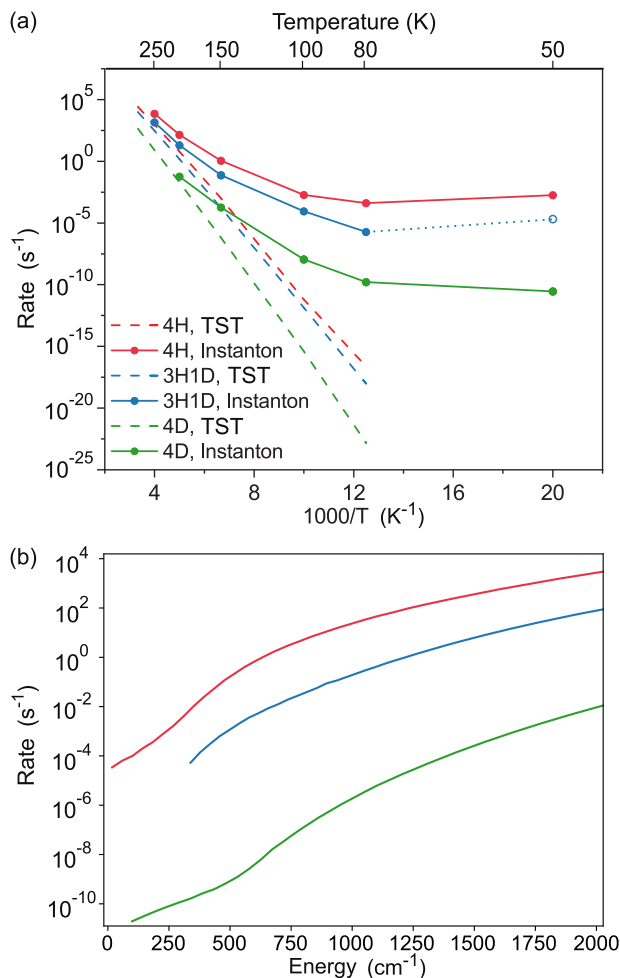


**FIG. 3.** (a) Canonical instanton rates. The temperature dependence of chirality switching rates. Due to numerical difficulties, the point marked with an open symbol could not reach our convergence criteria and is shown only for the purpose of a qualitative reference. (b) Microcanonical instanton rates. The red, blue, and green solid lines show the rates of chirality switching for 4H<sub>2</sub>O, 3H<sub>2</sub>O + D<sub>2</sub>O, and 4D<sub>2</sub>O, respectively.

Since thermal rate theories could not reach agreement with experimental findings, we consider the possibility that microcanonical rates are actually measured in the experiments instead of thermal rates. This is a possibility due to the extremely low temperature in the experimental setup and the electric current applied in the system for probing. We used the microcanonical instanton theory to compute the rate as a function of excitation energy instead of temperature. No additional instanton optimizations are required for this calculation; only post-processing of the instanton data are obtained for the thermal rate calculations. For each instanton (characterized with its energy  $E_I$ ), we compute  $W(E_I)$  and stability parameters<sup>42</sup> [which is required to compute  $Z_I(\beta; E_I)$ ]. Smooth functions of  $W(E_I)$  and the stability parameters (as functions of  $E_I$ ) are then obtained by spline interpolation over the discrete values. Finally,  $N_{\text{DoS}}(E)$  is obtained via numerical integration over the  $E_I$  grid [Eq. (8)] using Simpson's

**TABLE I.** Kink action  $S_{\text{kink}}/\hbar$  and tunneling splittings  $\Delta$  values for 4H<sub>2</sub>O, 3H<sub>2</sub>O + D<sub>2</sub>O, and 4D<sub>2</sub>O.

KIEs	$S_{\text{kink}}$	$\Delta$ (MHz)
4H <sub>2</sub> O	24.003	1.12
3H <sub>2</sub> O + 1D <sub>2</sub> O	26.288	0.017
4D <sub>2</sub> O	31.979	$2.08 \times 10^{-6}$

rule. One can obviously see from Fig. 3(b) that at any excitation energy, the rate for 3H<sub>2</sub>O + D<sub>2</sub>O is close to the rate for 4H<sub>2</sub>O, while being much higher than the rate for 4D<sub>2</sub>O. This trend is qualitatively the same as the trend in thermal rates [Fig. 3(a)] and in agreement with the Bell–Limbach model. Therefore, the conflict between theory and experiments does not result from energy excitation.

Finally, we use the instanton to compute the tunneling splittings in this system, an important quantity that have yet been studied. We calculate the kink actions and the tunneling splitting sizes of the 4H<sub>2</sub>O, 3H<sub>2</sub>O + D<sub>2</sub>O, and 4D<sub>2</sub>O systems, with the help of GPR to accelerate the optimization process. 150 beads are used and the kinks are optimized at 60 K for 4H<sub>2</sub>O and 3H<sub>2</sub>O + D<sub>2</sub>O, and at 40 K for 4D<sub>2</sub>O, with the *total force* on the instanton converged to below 0.06 eV/Å. The results are shown in Table I. The relative values of the tunneling splitting sizes upon partial and full deuteration show a similar trend to the rates, i.e., as Eq. (15), although it is for a completely different quantity. Partial deuteration suppresses the magnitude of this splitting, with the value being still detectable. Full deuteration, however, results in a value that is much smaller. We acknowledge that measuring these tunneling splitting sizes is extremely challenging in experiments. However, the consistent behavior of KIEs on tunneling splitting sizes and the tunneling rates at least presents an opportunity for future studies of the tunneling mechanism in experiments. However, we note that it is not clear whether experimental measurements of tunneling splittings of molecules adsorbed on surfaces are feasible or not.

## B. Porphycene

The second system where we have investigated the multiple PT process is porphycene. It is the first synthesized structural isomer of free base porphyrin, featuring unique intramolecular double PT dynamics.<sup>1,14,71,72</sup> In this double PT process, multiple TSs and meta-stable ISs exist. Same as the first-principles simulations for the former system, instanton theory is combined with on-the-fly electronic structure calculation with VASP. Different from the computational setup of the previous system, the hybrid functional B3LYP is employed for a better description of the PT process.<sup>73,74</sup> We note that the B3LYP function is still not accurate enough to reproduce the experiments,<sup>14,75</sup> but is suitable to predict qualitative results. The Brillouin zone was sampled using a single k-point. The potential energy profile of proton transfer in porphycene is summarized in Fig. 4, which shows that the protons transfer among the lowest four stationary points on the electronic ground-state potential energy surface. Previous electronic structure calculations have shown that the *trans* structure is the most stable tautomer of porphycene.<sup>76</sup> The energy of the *cis* structure is slightly higher than that of the *trans* (by 83 meV). The double proton transfer in porphycene has two pathways (concerted or stepwise), connecting the

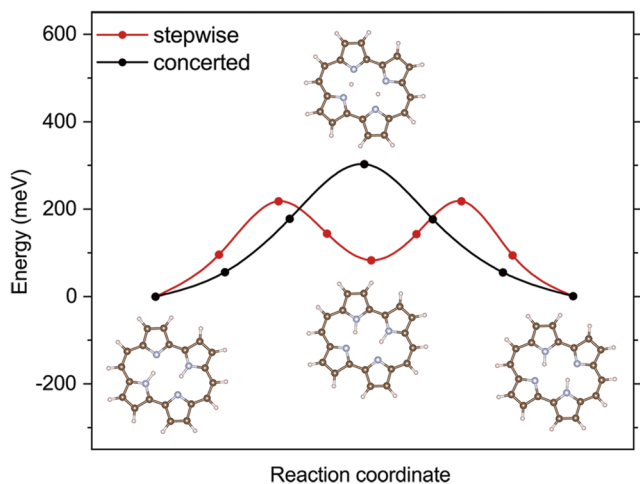


**FIG. 4.** Energy landscape of double proton transfer in porphycene. Black and red lines show the proton pathway through the concerted and stepwise mechanism, respectively. H, C, and N atoms are colored light pink, brown, and light gray, respectively.

two degenerate *trans* tautomeric states (Fig. 4). For concerted transfer, two protons move collectively through the second-order saddle point (the black curve in Fig. 4). For stepwise transfer, two protons move separately through *cis* configuration, which is the IS on the potential energy surface, a first-order saddle point. The barrier for concerted transfer is higher than that of the stepwise one.

Previous simulations have revealed that there is a competition between concerted and stepwise tunneling.<sup>14</sup> At high (low)  $T$ s, stepwise (concerted) tunneling is favored. At 100 K, the concerted path accounts for 95% of the total rate.<sup>14</sup> Our work focuses on the KIEs from partial and full deuteration. The tunneling rates at 100 K for the concerted and at 150 K for the stepwise mechanism are calculated for the HH, HD, and DD systems. In order to reduce the computational cost, we use a dual-level approach<sup>48</sup> to calculate instanton rates. Instanton optimizations and Hessian calculations are performed using the PBE functional. The potential energy along the tunneling path and the reactant state are recalculated using the hybrid functional B3LYP, which is used to correct the exponential part of the instanton rate. The results are shown in Fig. 5. It is clear that KIEs can distinguish between the concerted and stepwise mechanism. For concerted tunneling, partial deuteration decreases the rate. Full deuteration makes it substantially smaller. The evolution of  $k_{HH}$ ,  $k_{HD}$ , and  $k_{DD}$  agrees with Eq. (15). For stepwise tunneling, partial deuteration leads to an obvious decline in the tunneling rate, almost as the same level as full deuteration. The evolution of  $k_{HH}$ ,  $k_{HD}$ , and  $k_{DD}$  is in alignment with Eq. (14). These results, together with those of the water tetramer discussed above, corroborate the Bell–Limbach tunneling model for the KIEs in the concerted and stepwise PT rates.

The Bell–Limbach model has limitations regarding competing mechanisms. For gas phase porphycene, it has been shown that in the temperature range of 100–150 K, the rate for stepwise tunneling is comparable to the rate for concerted tunneling.<sup>14</sup> Here, we qualitatively discuss the behavior of KIEs in the overall rate for a

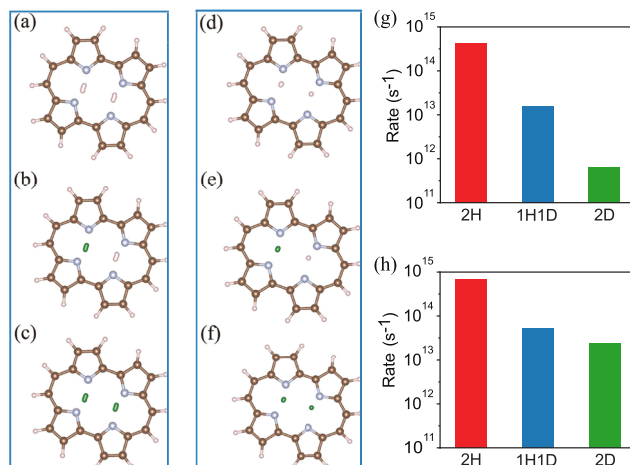


**FIG. 5.** Instanton paths and rates for concerted and stepwise tunneling in porphycene. [(a)–(c)] Concerted tunneling. The geometry of the instanton paths for 2H, 1H + 1D, and 2D. [(d)–(f)] Stepwise tunneling. The geometry of the instanton paths for 2H, 1H + 1D, and 2D. H, D, C, and N atoms are colored light pink, olive, brown, and light blue, respectively. (g) Concerted tunneling rates at 100 K. (h) Stepwise tunneling rates at 150 K.

system with two competing mechanisms. We make an assumption that  $k_{HH}/k_{HD}$  values for the two mechanisms are similar in the temperature range where the rate of the two mechanisms are comparable. One can see from Fig. 5 that  $k_{HH}/k_{HD}$  values for the two mechanisms are similar in the temperature range where the rates of the two mechanisms are comparable. In this case,  $k_{DD}$  for stepwise tunneling would be much larger than that for concerted tunneling, because the concerted tunneling rate decreases drastically going from partial to full deuteration. Therefore, the KIEs for the overall rate would be similar to the KIEs for the stepwise mechanism. This suggests that the observation of KIEs similar to the Bell–Limbach model for stepwise tunneling does not exclude the possibility that the system has a competition between stepwise and concerted tunneling mechanisms.

We note that the double PT process in the porphycene molecule on metal surfaces has been studied by STM experiments as well as instanton theory simulations.<sup>15,20,22,77,78</sup> Unlike porphycene in the gas-phase, DFT calculations predicted that the *cis* configuration is the most stable tautomer on Ag(110) and Cu(110) surfaces. On the Ag(110) surface, the *cis* to *cis* tautomerization via tunneling studied by STM shows that at 5 K, there is a large KIE of about 100 between HH- and DD-porphycene, while the KIE between DD- and HD-porphycene is only about two. According to the Bell–Limbach tunneling model, the *cis* to *cis* tautomerization of porphycene on Ag(110) occurs via a stepwise mechanism.<sup>20</sup> Theoretical simulations, however, clearly demonstrate a more competitive concerted tunneling mechanism at low  $T$ s and qualitatively different behaviors of partial and full deuteration.<sup>15</sup> Therefore, it is fair to say that theoretical simulations so far have presented a relatively consistent picture concerning the competition between stepwise and concerted tunneling in these systems.

Before concluding, we discuss other possible sources of the discrepancy between the experiments and theories. Previous studies

have already considered some important factors, for example, the influence of the height of the STM tip and alternative mechanisms, and concluded that these factors are unlikely to have any qualitative impact.<sup>21,61</sup> Apart from these factors, we do note that the STM tip may not be exactly at the center of the system, which could lead to the two chiral states not being equivalent. This could have some effect on the low temperature regime where deep tunneling through the bottom of the well occurs. Another plausible explanation is that there might be different interpretations of the signal measured in the STM experiment other than it being a proton transfer event. Finally, since the experiments are at very low temperatures ( $\sim 5$  K), if the coupling between the water tetramer and the substrate phonons is weak enough, it is possible that the tunneling phenomenon is coherent.<sup>79</sup> In this case, the observed rate could display different behaviors and could also depend on the frequency of measurement. Therefore, more efforts from both the theoretical and experimental sides are clearly desirable in the future.

#### IV. CONCLUSIONS

In this study, we investigate the KIEs and tunneling splittings in PT processes involving multiple protons with instanton theory, and with the help of machine learning assisted geometry optimization, which greatly reduced the computation cost of instanton optimizations at low temperatures. The systems studied cover two types of mechanisms, i.e., stepwise tunneling with meta-stable ISs and concerted tunneling. For both systems, our simulation results identified trends in the KIEs of the PT rates upon deuteration, which are qualitatively consistent with the Bell–Limbach model but inconsistent with recent experiments. We also considered the possibility that microcanonical rates were measured in the experiments instead of thermal rates due to the extremely low temperature and possible energy excitations from the probing current. However, the KIEs in the microcanonical tunneling rates also agree with the Bell–Limbach model. Given the significance of quantum tunneling in H-bonded systems, this study has a number of enlightening implications. It highlights some fundamental differences between the atomic level details of the stepwise and concerted tunneling mechanisms and their consequences. The corner-cutting effects mean that including the multi-dimensional feature of the proton transfer process can be important. Besides these, we point out that discrepancies between theory and experiments clearly remain, meaning that new theory/experiments are highly desirable.

#### ACKNOWLEDGMENTS

The authors thank Professor J. O. Richardson for the helpful discussions on this topic. Y.-H.C., Y.-C.Z., and X.-Z.L. were supported by the National Basic Research Programs of China under Grant Nos. 2017YFA0205003 and 2021YFA1400503, the National Science Foundation of China under Grant No. 11934003, the Beijing Natural Science Foundation under Grant No. Z200004, and the Strategic Priority Research Program of the Chinese Academy of Sciences under Grant No. XDB33010400. The computational resources were provided by the supercomputer center in Peking University, China.

#### AUTHOR DECLARATIONS

##### Conflict of Interest

The authors have no conflicts of interest to disclose.

##### DATA AVAILABILITY

The data that support the findings of this study are available from the corresponding author upon reasonable request.

#### REFERENCES

- 1 D. Sánchez-García and J. L. Sessler, *Chem. Soc. Rev.* **37**, 215 (2008).
- 2 J. Chen, J. Guo, X. Meng, J. Peng, J. Sheng, L. Xu, Y. Jiang, X. Z. Li, and E. G. Wang, *Nat. Commun.* **5**, 4056 (2014).
- 3 C. Drechsel-Grau and D. Marx, *Phys. Chem. Chem. Phys.* **19**, 2623 (2017).
- 4 L. E. Bove, S. Klotz, A. Paciaroni, and F. Sacchetti, *Phys. Rev. Lett.* **103**, 165901 (2009).
- 5 M. Benoit, D. Marx, and M. Parrinello, *Nature* **392**, 258 (1998).
- 6 M. Ceriotti, W. Fang, P. G. Kusalik, R. H. McKenzie, A. Michaelides, M. A. Morales, and T. E. Markland, *Chem. Rev.* **116**, 7529 (2016).
- 7 T. E. Markland and M. Ceriotti, *Nat. Rev. Chem.* **2**, 0109 (2018).
- 8 C. Drechsel-Grau and D. Marx, *Phys. Rev. Lett.* **112**, 148302 (2014).
- 9 S. Maier, I. Stass, J. I. Cerdá, and M. Salmeron, *Phys. Rev. Lett.* **112**, 126101 (2014).
- 10 O. Benton, O. Sikora, and N. Shannon, *Phys. Rev. B* **93**, 125143 (2016).
- 11 C. Drechsel-Grau and D. Marx, *Angew. Chem., Int. Ed.* **53**, 10937 (2014).
- 12 B. Pamuk, J. M. Soler, R. Ramírez, C. P. Herrero, P. W. Stephens, P. B. Allen, and M.-V. Fernández-Serra, *Phys. Rev. Lett.* **108**, 193003 (2012).
- 13 W. Fang, J. Chen, M. Rossi, Y. Feng, X.-Z. Li, and A. Michaelides, *J. Chem. Phys.* **7**, 002125 (2016).
- 14 Y. Litman, J. O. Richardson, T. Kumagai, and M. Rossi, *J. Am. Chem. Soc.* **141**, 2526 (2019).
- 15 Y. Litman and M. Rossi, *Phys. Rev. Lett.* **125**, 216001 (2020).
- 16 D. Gerbig and P. R. Schreiner, *Angew. Chem., Int. Ed.* **56**, 9445 (2017).
- 17 K. T. Wikfeldt and A. Michaelides, *J. Chem. Phys.* **140**, 041103 (2014).
- 18 C. J. Jameson, *Chem. Rev.* **91**, 1375 (1991).
- 19 K. Jackowski and M. Jaszunski, *Gas Phase NMR* (Royal Society of Chemistry, London, 2016).
- 20 M. Koch, M. Pagan, M. Persson, S. Gawinkowski, J. Waluk, and T. Kumagai, *J. Am. Chem. Soc.* **139**, 12681 (2017).
- 21 X. Meng, J. Guo, J. Peng, J. Chen, Z. Wang, J.-R. Shi, X.-Z. Li, E.-G. Wang, and Y. Jiang, *Nat. Phys.* **11**, 235 (2015).
- 22 T. Kumagai, J. N. Ladenthin, Y. Litman, M. Rossi, L. Grill, S. Gawinkowski, J. Waluk, and M. Persson, *J. Chem. Phys.* **148**, 102330 (2018).
- 23 A. P. Jardine, E. Y. M. Lee, D. J. Ward, G. Alexandrowicz, H. Hedgeland, W. Allison, J. Ellis, and E. Pollak, *Phys. Rev. Lett.* **105**, 136101 (2010).
- 24 A. Tuladhar, S. M. Piontek, and E. Borguet, *J. Phys. Chem. C* **121**, 5168 (2017).
- 25 M. Sovago, R. Kramer Campen, H. J. Bakker, and M. Bonn, *Chem. Phys. Lett.* **470**, 7 (2009).
- 26 L. Fu, D. Xiao, Z. Wang, V. S. Batista, and E. C. Y. Yan, *J. Am. Chem. Soc.* **135**, 3592 (2013).
- 27 X. Huang, J. Nelson, J. Kirz, E. Lima, S. Marchesini, H. Miao, A. M. Neiman, D. Shapiro, J. Steinbrener, A. Stewart, J. J. Turner, and C. Jacobsen, *Phys. Rev. Lett.* **103**, 198101 (2009).
- 28 J. Meisner, J. B. Rommel, and J. Kästner, *J. Comput. Chem.* **32**, 3456 (2011).
- 29 T.-S. Lin and R. Gomer, *Surf. Sci.* **255**, 41 (1991).
- 30 L. J. Lauhon and W. Ho, *Phys. Rev. Lett.* **85**, 4566 (2000).
- 31 W. Fang, J. O. Richardson, J. Chen, X.-Z. Li, and A. Michaelides, *Phys. Rev. Lett.* **119**, 126001 (2017).
- 32 X. D. Zhu, A. Lee, A. Wong, and U. Linke, *Phys. Rev. Lett.* **68**, 1862 (1992).
- 33 J. O. Richardson and S. C. Althorpe, *J. Chem. Phys.* **131**, 214106 (2009).

- <sup>34</sup>S. Andersson, G. Nyman, A. Arnaldsson, U. Manthe, and H. Jónsson, *J. Phys. Chem. A* **113**, 4468–4478 (2009).
- <sup>35</sup>J. Kästner, *Wiley Interdiscip. Rev.: Comput. Mol. Sci.* **4**, 158 (2014).
- <sup>36</sup>J. O. Richardson, *J. Chem. Phys.* **148**, 200901 (2018).
- <sup>37</sup>J. O. Richardson, *Int. Rev. Phys. Chem.* **37**, 171 (2018).
- <sup>38</sup>J. Guo, “Concerted proton tunneling,” in *High Resolution Imaging, Spectroscopy and Nuclear Quantum Effects of Interfacial Water* (Springer, Singapore, 2018), pp. 83–94.
- <sup>39</sup>H.-H. Limbach, J. Hennig, D. Gerritzen, and H. Rumpel, *Faraday Discuss.* **74**, 229 (1982).
- <sup>40</sup>H.-H. Limbach, J. Miguel Lopez, and A. Kohen, *Philos. Trans. R. Soc., B* **361**, 1399 (2006).
- <sup>41</sup>H. Eyring, *J. Chem. Phys.* **3**, 107 (1935).
- <sup>42</sup>W. H. Miller, *J. Chem. Phys.* **62**, 1899 (1975).
- <sup>43</sup>J. O. Richardson, *J. Chem. Phys.* **144**, 114106 (2016).
- <sup>44</sup>M. Kryvohuz, *J. Chem. Phys.* **134**, 114103 (2011).
- <sup>45</sup>Z. Smedarchina, W. Siebrand, and A. Fernández-Ramos, *J. Chem. Phys.* **137**, 224105 (2012).
- <sup>46</sup>J. O. Richardson, *Faraday Discuss.* **195**, 49 (2016).
- <sup>47</sup>P. Winter and J. O. Richardson, *J. Chem. Theory Comput.* **15**, 2816 (2019).
- <sup>48</sup>J. Meisner and J. Kästner, *J. Chem. Theory Comput.* **14**, 1865 (2018).
- <sup>49</sup>M. Ceotto, *Mol. Phys.* **110**, 547 (2012).
- <sup>50</sup>M. J. Gillan, *J. Phys. C: Solid State Phys.* **20**, 3621 (1987).
- <sup>51</sup>V. A. Benderskii, D. E. Makarov, and C. A. Wight, “Chemical dynamics at low temperatures,” in *Advances in Chemical Physics* (Wiley, New York, 1994), Vol. 88.
- <sup>52</sup>R. A. Marcus and O. K. Rice, *J. Phys. Chem.* **55**, 894 (1951).
- <sup>53</sup>J. I. Steinfeld, J. S. Francisco, and W. L. Hase, *Chemical Kinetics and Dynamics*, 2nd ed. (Prentice Hall, Upper Saddle River, NJ, 1989).
- <sup>54</sup>S. Chapman, B. C. Garrett, and W. H. Miller, *J. Chem. Phys.* **63**, 2710 (1975).
- <sup>55</sup>S. R. McConnell, A. Löhle, and J. Kästner, *J. Chem. Phys.* **146**, 074105 (2017).
- <sup>56</sup>W. Fang, P. Winter, and J. O. Richardson, *J. Chem. Theory Comput.* **17**, 40 (2021).
- <sup>57</sup>R. P. Bell, *The Tunnel Effect in Chemistry* (Chapman and Hall, London, 1980).
- <sup>58</sup>J. O. Richardson and S. C. Althorpe, *J. Chem. Phys.* **134**, 054109 (2011).
- <sup>59</sup>G. Laude, D. Calderini, D. P. Tew, and J. O. Richardson, *Faraday Discuss.* **212**, 237 (2018).
- <sup>60</sup>O.-P. Koistinen, F. B. Dagbjartsdóttir, V. Ásgeirsson, A. Vehtari, and H. Jónsson, *J. Chem. Phys.* **147**, 152720 (2017).
- <sup>61</sup>Y. Feng, Z. Wang, J. Guo, J. Chen, E.-G. Wang, Y. Jiang, and X.-Z. Li, *J. Chem. Phys.* **148**, 102329 (2018).
- <sup>62</sup>C. Drechsel-Grau and D. Marx, *Nat. Phys.* **11**, 216 (2015).
- <sup>63</sup>O. Klein, F. Aguilar-Parrilla, J. M. Lopez, N. Jagerovic, J. Elguero, and H.-H. Limbach, *J. Am. Chem. Soc.* **126**, 11718 (2004).
- <sup>64</sup>I. R. Craig and D. E. Manolopoulos, *J. Chem. Phys.* **123**, 034102 (2005).
- <sup>65</sup>R. Colleparado-Guevara, I. R. Craig, and D. E. Manolopoulos, *J. Chem. Phys.* **128**, 144502 (2008).
- <sup>66</sup>G. Kresse and J. Hafner, *Phys. Rev. B* **47**, 558 (1993).
- <sup>67</sup>G. Kresse and J. Hafner, *Phys. Rev. B* **49**, 14251 (1994).
- <sup>68</sup>J. P. Perdew, K. Burke, and M. Ernzerhof, *Phys. Rev. Lett.* **77**, 3865 (1996).
- <sup>69</sup>S. Grimme, *J. Comput. Chem.* **27**, 1787 (2006).
- <sup>70</sup>G. Henkelman, B. P. Uberuaga, and H. Jónsson, *J. Chem. Phys.* **113**, 9901 (2000).
- <sup>71</sup>J. Waluk, *Chem. Rev.* **117**, 2447 (2017).
- <sup>72</sup>P. Fita, N. Urbanska, C. Radzewicz, and J. Waluk, *Chem. - Eur. J.* **15**, 4851 (2009).
- <sup>73</sup>A. D. Becke, *J. Chem. Phys.* **98**, 5648 (1993).
- <sup>74</sup>C. Lee, W. Yang, and R. G. Parr, *Phys. Rev. B* **37**, 785 (1988).
- <sup>75</sup>P. Ciałka, P. Fita, A. Listkowski, C. Radzewicz, and J. Waluk, *J. Phys. Chem. Lett.* **7**, 283 (2016).
- <sup>76</sup>T. Yoshikawa, S. Sugawara, T. Takayanagi, M. Shiga, and M. Tachikawa, *Chem. Phys. Lett.* **496**, 14 (2010).
- <sup>77</sup>T. Kumagai, F. Hanke, S. Gawinkowski, J. Sharp, K. Kotsis, J. Waluk, M. Persson, and L. Grill, *Nat. Chem.* **6**, 41 (2014).
- <sup>78</sup>T. Kumagai, *Prog. Surf. Sci.* **90**, 239 (2015).
- <sup>79</sup>A. Vdovin, J. Waluk, B. Dick, and A. Slenczka, *ChemPhysChem* **10**, 761 (2009).